

FABRICATION AND CHARACTERIZATION OF Mn-CdS NANOPATES AND THEIR PHOTOCATALYTIC PERFORMANCES

L. XU^{a*}, X.T. NING^b

^a*College of Mechanical Engineering, Hunan University of Arts and Science, Changde 415000, People's Republic of China*

^b*Hunan University of Humanities, Science and Technology, School of Environmental and Materials Engineering*

Graphene/Mn-doped CdS nanoplates (G/Mn-CdS NP) composite photocatalysts were prepared via a microwave-assisted method and characterized via XRD, UV-Vis spectroscopy, XPS, SEM, TEM, and HRTEM. The as-prepared G/Mn-CdS NP composite displayed a maximum photodegradation of methylene orange dye of 79.7% under visible light irradiation. The unique nanoplate structure, graphene support, and Mn²⁺ doping in the nanocomposite induced synergistic effects in its photocatalytic performance, which enhanced its charge transfer, improved its light utilization, and suppressed the recombination of photogenerated electron-hole pairs. Such composite photocatalysts are expected to have great practical applications for environmental remediation.

(Received February 3, 2020; Accepted June 5, 2020)

Keywords: Graphene, Doped, Photocatalytic performance

1. Introduction

Semiconductor photocatalysts have an extensive range of applications in environmental remediation[1]. Cadmium sulfide (CdS) is an appropriate semiconductor for such photocatalysts since it has a suitable band gap (2.4 eV) for absorbing visible light and a more negative conduction band edge[2]. Controlling the shape of semiconductor nanomaterials has been proven to be an effective method to harvest and harness solar energy for practical applications[3]. Nanoplates have a fast charge carrier mobility and a high light-harvesting efficiency, which can help obtain superior catalytic activities[4]. However, the fast charge recombination of photogenerated electrons and holes greatly restricts their applications in environmental remediation[5].

To overcome these problems, various carbon-based composites have been developed and used as catalysts with large surface areas and high carrier mobilities. In particular, graphene-based composites are highly attractive compared with other carbon-containing CdS-materials[6]. The assembly of nanocomposites using graphene can facilitate charge carrier migration, reduce the recombination rate, enhance visible light absorption, and improve pollutant adsorption, all of which can increase the photo-efficiency[7]. Additionally, metal-ion doping has proven to be a valid method for extending the lifetime of charge carriers. In materials doped with Mn²⁺ ions, photoinduced electrons in the conduction band of CdS are easily transferred to Mn²⁺ energy levels, which act as electron traps and prevents the recombination of electron-hole pairs[8]. However, there are no reports on Mn²⁺ doped CdS nanoplates combined with graphene and their photocatalytic performance.

Thus, in this work, we report the assembly and visible light photocatalytic performance of Mn²⁺-doped CdS nanoplates containing graphene.

2. Experimental details

2.1. Preparation of G/Mn-CdS NP

In a typical procedure, 0.05 g of graphene oxide, 0.1 mmol of manganese (II) acetate

* Corresponding author: 21467855@qq.com

tetrahydrate ($C_4H_{14}MnO_8 \cdot 4H_2O$), 4 mmol of cadmium acetate dihydrate ($Cd(AC)_2 \cdot 2H_2O$), and 4 mmol of thioacetamide (H_2NCSNH_2GSH) were dissolved in a mixed solution containing 50% deionized water and 50% ethylene glycol ($C_2H_6O_2$, $\geq 99.9\%$ purity, Aladdin). After constant stirring for 1 h, the solution was transferred into a microwave chemical reactor and held at 180 °C for 30 min. The obtained precipitates were washed with de-ionized water several times to remove unreacted chemicals and then dried at 80 °C.

2.2. Characterization

The morphology and microstructure of the products were analyzed with scanning electron microscopy (SEM, S4800) and transmission electron microscopy (TEM, JEM-2100F). X-ray photoelectron spectroscopy (XPS) was performed on an X-ray photoelectron spectrometer (K-alpha 1063). The crystal structure and phase purity of the as-prepared products were characterized by X-ray diffraction (D5000) using Cu $K\alpha$ radiation. UV-vis absorption spectra were analyzed by a UV-vis spectrometer (UV-2550, SHIMADZU, Japan).

2.3. Photocatalytic experiments

Photocatalytic activities were evaluated by monitoring the photodegradation of methyl orange (MO) under visible light irradiation. A typical experiment involved adding 0.1 g of photocatalyst to 100 mL of 10 mg/L MO aqueous solution in a photo-reactor vessel and stirring in the dark for 30 min to reach adsorption equilibrium. Solutions were irradiated with visible light using a 250 W xenon lamp with a cutoff filter (>420 nm). Every 20 min, 5 mL of the suspension was sampled and centrifuged, and then UV-Vis spectra were recorded on a UV-Vis spectrophotometer (UV-2550).

2. Results and discussion

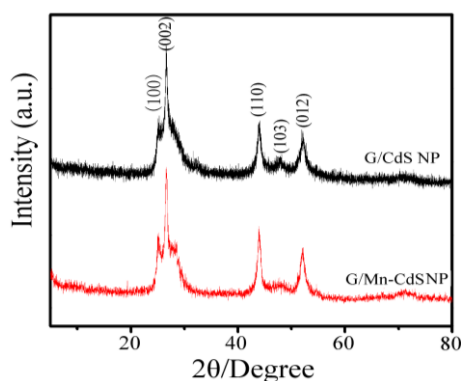


Fig. 1. XRD of the samples.

The phases and structures of materials are investigated by X-ray diffraction. As shown in Fig. 1, the G/CdS NP and G/Mn-CdS NP samples had similar spectra, and all diffraction peaks were indexed to hexagonal CdS (no. 77-2306). The lack of a manganese signal indicated that manganese doping did not change the main crystal structure of CdS[9]. However, the peak intensity of G/Mn-doped CdS was obviously stronger than that of G/CdS NP, demonstrating the good crystallization of CdS after Mn-doping[10]. Additionally, the lack of obvious graphene peaks indicated that the graphene was well-dispersed in the nanocomposites[11].

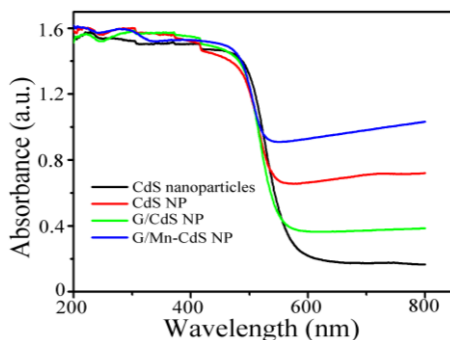


Fig. 2. UV-visible spectroscopy of the samples.

UV-visible spectroscopy is useful for evaluating the photoresponse of samples, and a strong absorption in the visible region was observed in all samples (Fig. 2), which was attributed to the intrinsic band gap of CdS. G/Mn-CdS NP showed the highest absorbance of all samples, which clearly suggested that combining the nanoplates with graphene and Mn-doping produced a superior visible light absorption, which was favorable for photocatalytic reactions[12].

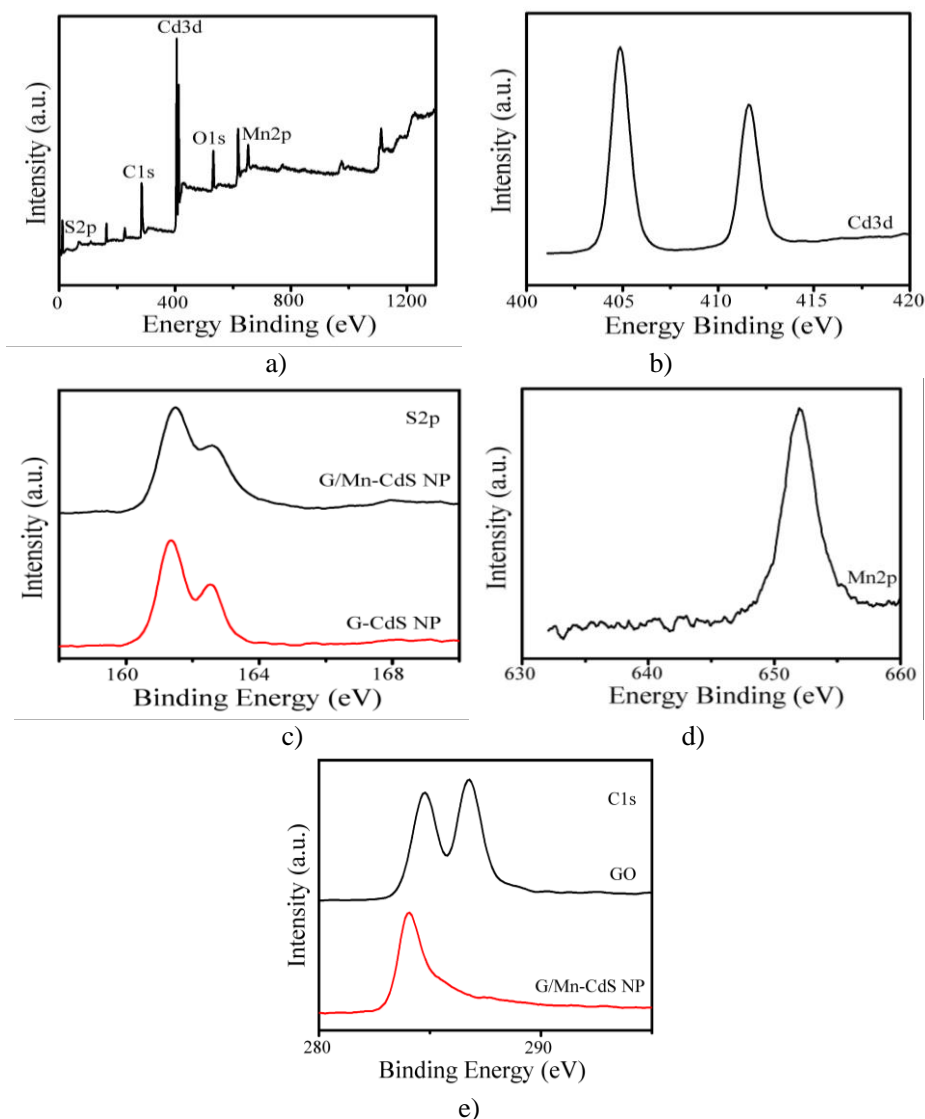


Fig. 3. Typical XPS spectra of the samples: (a) survey spectra, (b) Cd3d region XPS spectrum, (c) S 2 p region XPS spectrum, (d) Mn 2p s region XPS spectrum, (e) C 1s region XPS spectrum.

The elemental composition of G/Mn-CdS NP is analyzed by X-ray photoelectron spectroscopy (XPS). The typical XPS survey spectrum in Fig. 3a clearly showed peaks of C1s, Cd 3d, S 2p, Mn 2p, and O1s, confirming the presence of C, Cd, Mn, S, and O. Fig. 3b showed the peaks of Cd (Cd 3d_{5/2}, 404.88 eV; Cd 3d_{3/2}, 411.58 eV). The binding energies (161.48 and 162.58 eV) representing the 2p_{3/2} and 2p_{1/2} states of S2p in G/Mn-doped CdS NP were higher than G/CdS NP (161.33 eV and 162.53 eV, respectively), most likely due to the incorporation of Mn ions in the CdS lattice, which formed Cd-S-Mn bonds. The peak at 651.98 eV was assigned to Mn 2p_{1/2} of Mn²⁺ ions which was similar to Mn²⁺ in MnS, indicating that Cd²⁺ was replaced by Mn²⁺ in the CdS lattice[13]. Fig. 2e showed the C 1s XPS spectrum of GO (graphene oxides) and G/Mn-CdS NP. Compared with GO, oxygenated functional groups (O-C=O, 286.78 eV) were drastically decreased and the C=C-C peak (284.78 eV) was the dominant peak in the G/Mn-CdS NP pattern, indicating that efficient electron transport ability could be realized[14].

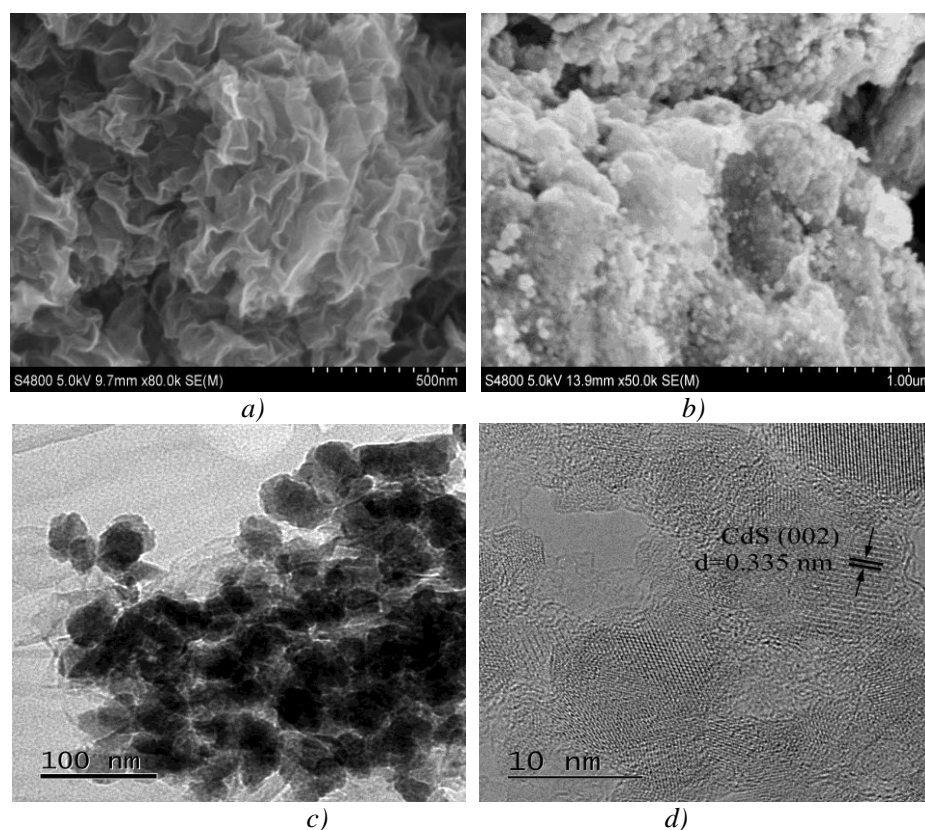


Fig. 4. (a) SEM image of GO, (b) SEM, (c) TEM (d) HRTEM of G/Mn-CdS NP.

The typical morphologies of GO and G/Mn-CdS NP are characterized by SEM, TEM, and HRTEM. Fig. 4a showed that GO has a gauze-like morphology, and after the formation of G/Mn-CdS NP (Fig. 4b), it could be seen that graphene resembled crumpled sheets, and uniformly-shaped CdS nanoplates were coated on its surface. The TEM image in Fig. 4c further showed the plate-shaped structure of CdS with a diameter of around 50 nm, which was in contact with the graphene surface. The high-resolution TEM image (Fig. 4d) revealed the clear crystallinity of CdS with a lattice spacing of 0.335 nm, corresponding to the (002) planes of hexagonal CdS[15].

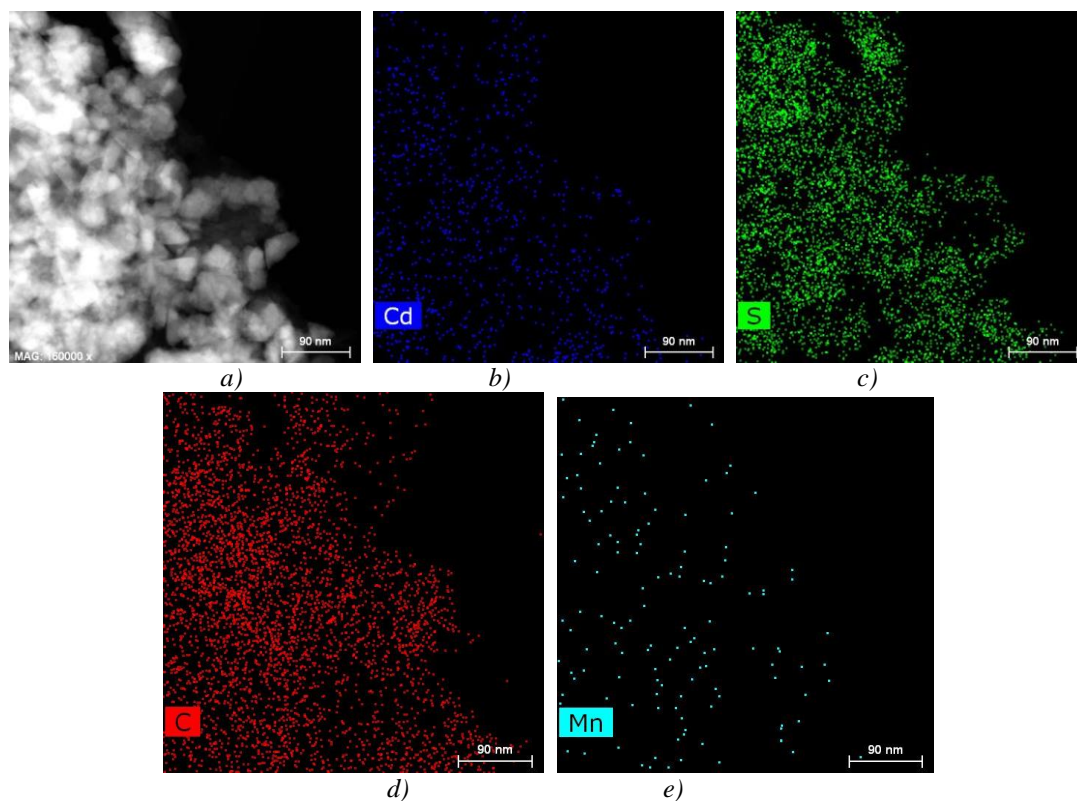


Fig. 5. (a)TEM of EDS mapping of selected area, (b) element Cd mapping, (c) element S mapping, (d) element C mapping, (e) element Mn mapping of G/Mn-CdS.

EDS maps of a selected area (Fig. 5) demonstrated the uniform distribution of Cd, S, and C throughout the nanomesh structure, indicating the successful formation of graphene and CdS nanoplates. Furthermore, the Mn distribution was consistent with that of Cd and S elements, indicating that Mn ions were firmly incorporated into the CdS lattice[16].

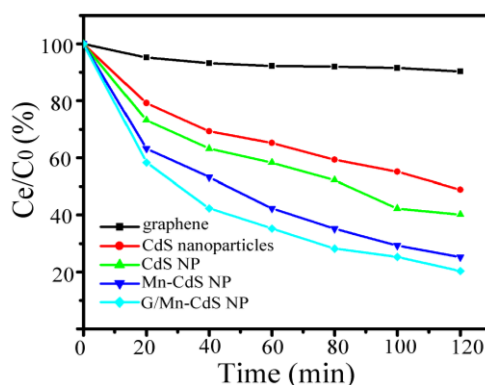
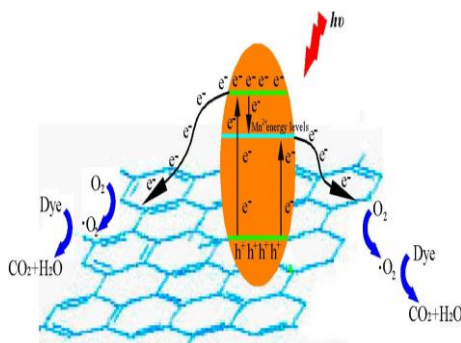


Fig. 6. Photocatalytic degradation efficiency of MO with different catalysts under visible light.

The photocatalytic properties of the photocatalysts are evaluated by measuring the photodegradation of MO, as shown in Fig. 6. Clearly, the addition of graphene under visible light irradiation did not lead to the decolorization of MO (<10%) after 120 min. In contrast, for the same irradiation time, the degradation efficiency reached 51.1%, 59.8%, 74.8%, and 79.7% when using CdS nanoparticles, CdS NP, Mn-CdS NP, and G/Mn-CdS NP, respectively. The superior photodegradation performance of G/Mn-CdS NP was due to synergetic effects in which the CdS

nanoplates provided more active sites, Mn-doped CdS induced high charge separation, and graphene increased the light-harvesting efficiency[17].



Scheme 1. Schematic illustration for the charge transfer and separation in the G/Mn-CdS NP system.

The following mechanism can be proposed for G/Mn-CdS NP. New Mn²⁺ energy levels emerges in the bandgap of CdS with respect to that of G/CdS NP[13]. Under visible light irradiation, electrons (e⁻) are excited to the conduction band (CB) of CdS or to the newly-formed Mn²⁺ energy levels. The electrons in the CB of CdS could also transfer to Mn²⁺ energy levels[13]. The photoexcited electrons in the CB of CdS and Mn²⁺ energy levels could both be transferred to graphene, which effectively hinders the recombination of photogenerated electron-hole pairs. Finally, these photogenerated electrons in graphene can react with O₂ to produce $\cdot\text{O}_2^-$, which degrade the dye into CO₂, H₂O, and other small molecules[18].

4. Conclusions

In summary, we have demonstrated the synthesis of Mn-doped CdS nanoplates decorated with graphene via a microwave method. The as-prepared composite exhibited superior photocatalytic performance toward MO photodegradation, which was closely related to the nanoplate structure, graphene, as well as Mn²⁺ doping. The nanoplate structure may favor fast charge carrier mobility. The graphene and the newly-formed Mn²⁺ energy levels enhanced the visible light absorption and reduced the recombination rate of photo-generated carriers. This work may provide a new method to rationally design environmental remediation photocatalysts.

References

- [1] C. S. Chen, X. Y. Liu, H. Long et al., *Vacuum*. **164**, 66 (2019).
- [2] L. Cheng, Q. J. Xiang, Y. L. Liao et al., *Energ. Environ. Sci.* **11**, 1362 (2018).
- [3] B. Zhang, W. F. Yao, C. P. Huang et al., *Int. J. Hydrogen Energ.* **38**(18), 7224 (2013).
- [4] Y. Xiao, C. S. Chen, S. Y. Cao et al., *Ceram. Int.* **41**, 10087 (2015).
- [5] Y. K. Zhang, Z. L. Jin, *Phys. Chem. Chem. Phys.* **21**, 8326 (2019).
- [6] W. W. Yu, X. A. Chen, W. Mei et al., *Appl. Surf. Sci.* **400**, 129 (2017).
- [7] W. Mei, M. Lin, C. S. Chen et al., *J Nanopart. Res.* **20**(11), 286 (2018).
- [8] C. Y. Zhang, J. S. Lai, J. C. Hu, *RSC Adv.* **5**, 15110 (2015).
- [9] M. Karolewicz, H. Fuks, E. Tomaszewicz, *J. Therm. Anal. Calorim.* **138**, 2219 (2019).
- [10] X. C. Lv, C. Y. Hu, J. Shang et al. *Cataly. Today*. **335**, 468 (2019).
- [11] B. Zeng, W. Liu, W. Zeng et al., *Chalcogenide Lett.* **16**(2), 73 (2019).
- [12] M. Z. Rahaman, A. K. Hossain, *RSC Adv.* **8**, 33010 (2018).
- [13] B. Zeng, W. Zeng, *Dig. J Nanomater. Bios.* **14**(3), 627 (2019).
- [14] B. Zeng, W. Zeng, *Dig. J Nanomater. Bios.* **12**(1), 27 (2017).
- [15] X. Gao, X. X. Liu, Z. M. Zhu, et al. *Sci. Rep.* **7**, 973 (2017).

- [16] X. D. Yang, G. G. Lu, B. Y. Wang et al., *RSC Adv.* **9**, 25142 (2019).
- [17] L. Jia, D. H. Wang, Y. X. Huang et al., *J. Phys. Chem. C* **115**(23), 11466 (2011).
- [18] B. Zeng, X. Chen. *J. Nanomater., Bios.* **11**(2), 559 (2016).